Expert Systems With Applications 236 (2024) 121371

Contents lists available at ScienceDirect

Expert Systems With Applications

journal homepage: www.elsevier.com/locate/eswa

Molecular subtypes classification of breast cancer in DCE-MRI using deep features

Ali M. Hasan [a,*], Noor K.N. Al-Waely [a], Hadeel K. Aljobouri [b], Hamid A. Jalab [c,d], Rabha W. Ibrahim [d,e,f], Farid Meziane [g]

[a] College of Medicine, Al-Nahrain University, Baghdad, Iraq
[b] Biomedical Engineering Department, College of Engineering, Al-Nahrain University, Iraq
[c] Faculty of Computer Science and Information Technology, University of Malaya, 50603 Kuala Lumpur, Malaysia
[d] Information and Communication Technology Research Group, Scientific Research Center, Al-Ayen University, Nile Street, 64001 Thi-Qar, Iraq
[e] Department of Computer Science and Mathematics, Lebanese American University, Beirut 1102 2801, Lebanon
[f] Near East University, Mathematics Research Center, Department of Mathematics, Near East Boulevard, PC: 99138, Nicosia/Mersin 10, Turkey
[g] Data Science Research Centre, School of Computing and Engineering, University of Derby, United Kingdom

ARTICLE INFO

Keywords:
Molecular subtypes
Breast cancer
DCE-MRI
Classification
Deep learning

ABSTRACT

Breast cancer is a major cause of concern on a global scale due to its high incidence rate. It is one of the leading causes of death for women, if left untreated. Dynamic contrast-enhanced magnetic resonance imaging (DCE-MRI) is increasingly being used in the evaluation of breast cancer. Prior studies neglected to take into account breast cancer characteristics and features that might be helpful for distinguishing the four molecular subtypes of breast cancer. The use of breast DCE-MRI to identify the molecular subtypes is now the focus of research in breast cancer analysis. It offers breast cancer patients a better chance for an early and effective treatment plan. A manually annotated dataset of 1359 DCE-MRI images was used in this study, with 70% used for training and the remaining for testing. Twelve deep features were extracted from this dataset. The dataset was initially pre-processed through placing the ROIs by a radiologist experienced in breast MRI interpretation, then deep features are extracted using the proposed convolutional neural network (CNN). Finally, the deep features extracted are classified into molecular subtypes of breast cancer using the support vector machine (SVM). The effectiveness of the predictive model was assessed using accuracy and area under curve (AUC) measures. The test was performed on unseen held-out data. The maximum achieved accuracy and AUC were 99.78% and 100% respectively, with substantially a low complexity rate.

1. Introduction

Breast cancer can affect both men and women, but it is more common in women, and it is the second leading cause of cancer-related deaths globally (Sung et al., 2021). In 2022, the Iraqi cancer board from the Ministry of Health (MOH) has reported that between 2000 and 2019, nearly 70,000 women received a breast cancer diagnosis (Al-Hashimi, 2021). The World Health Organization (WHO) reported that breast cancer treatment can be highly effective, especially when the cancer is detected in early stages by screening tests (Hasan et al., 2022). Screening and early diagnosis of breast cancer by a non-invasive imaging modality such as mammography, magnetic resonance imaging (MRI), ultrasound, etc., can significantly affect patient's prognosis and prevent cancer spreading outside of the breast (Li et al., 2019).

Breast cancer develops when breast cells grow abnormally resulting in a mass of tissue known as a tumor. Like other cancers, breast cancer can invade other healthy breast tissues, and can travel through the blood stream to the lymph nodes in the axilla and to other parts of the body (Feng et al., 2018). There are many symptoms for breast cancer and these vary form woman to woman, but the first observable symptom, in addition to breast pain, skin changes, nipple discharge, and obvious changes in the size and shape of the breast, is typically a lump or area of thickened breast tissue. However, a lot of breast cancers are undetectable without the aid of breast imaging techniques. The selection of an

* Corresponding author.
E-mail addresses: alialwaeli@nahrainuniv.edu.iq (A.M. Hasan), noor83kadhem@nahrainuniv.edu.iq (N.K.N. Al-Waely), hadeel.k.aljobouri@nahrainuniv.edu.iq (H.K. Aljobouri), hamidjalab@um.edu.my (H.A. Jalab), rabhawaell.ibrahim@lau.edu.lb, rabhawaell.ibrahim@neu.edu.tr (R.W. Ibrahim), F.Meziane@derby.ac.uk (F. Meziane).

https://doi.org/10.1016/j.eswa.2023.121371
Received 20 March 2023; Received in revised form 11 August 2023; Accepted 27 August 2023
Available online 1 September 2023

imaging technique for a patient's diagnosis of breast cancer depends on the patient's age and the density of breast tissue (Iranmakani et al., 2020). Three breast imaging modalities are currently employed in the evaluation of breast lesions. The first standard imaging modality to examine the breasts, is the mammography. It is considered the gold standard imaging modality in population-based breast cancer screening programs, and it is routinely used in the characterization of breast pathologies. However, for certain types of breasts, mammograms can be challenging to interpret as dense breasts are difficult to scrutinize and lesions can be obscured (Iranmakani et al., 2020; Zhao et al., 2015). The second imaging modality is ultrasonography (US). Although US examination entails the ability to diagnose breast abnormalities without ionizing radiation, it has many limitations including: many breast cancers are not visible on US, and most of US-detected suspicious findings require biopsy (Lee & Houssami, 2016).

The third imaging modality is MRI, which is a well-recognized imaging study used for screening patient with high risk of developing breast cancer, characterization of an indeterminate breast lesion, and in cases of biopsy proven cancer for pre-operative assessment and surgical planning (Zhang et al., 2021). In MRI, a number of radio frequency pluses and gradients are used to characterize tissues by different relaxation times to produce various pulse sequences including T1 and T2 sequences with particular appearance of breast tissues on each sequence (Blink, 2004). By considering the information provided by these MRI pulse sequences, useful data for breast lesion diagnosis can be extracted (Kawahara & Nagata, 2021). In most breast MRI protocols gadolinium contrast medium is routinely administered. After the gadolinium is injected, the signal intensity in the vessels and certain breast lesions is increased rapidly, then followed by a washout of contrast due to diffusion into the interstitial space. By tracking the diffusion of the contrast material over time, it can study microvascular structure in vivo using DCE-MRI technique (Ferris & Goergen, 2016; Ulas et al., 2019). DCE-MRI is non-invasive and effective imaging technique that collects a series of T1 weighted images at intervals of few seconds repeatedly over the entire coverage of the suspected lesion volume during the intravenous injection of gadolinium to study the extent and characteristics of the microvasculature in many physiological and pathological instances. It has been validated as potential biomarkers which can give insight into the biological processes in breast cancer development, understand molecular subtypes of breast cancer, and help the clinicians to build better treatment plans (Li et al., 2019; Omer et al., 2019; Ulas et al., 2019).

To this moment, the growth and spread of breast cancer has not been fully understood because cancer cells growth is fueled by normal healthy hormones: estrogen and progesterone that keep the female reproductive system healthy. Some of the breast cancers are sensitive to these normal hormones; where, breast cancer cells have receptors on the outside of their cell walls that can bind to specific hormones that circulate throughout the body. Progesterone receptor (PR), estrogen receptor (ER), and human epidermal growth factor receptor 2 (HER2), which are also known as growth receptors, to mediate cancer cell growth signaling as shown in Fig. 1.

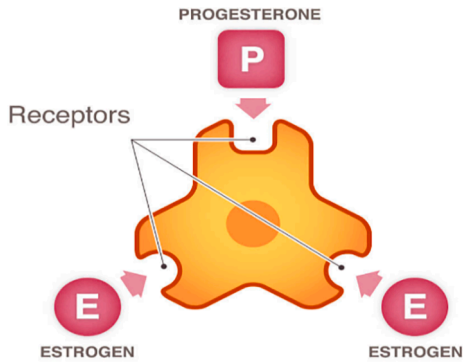

Fig. 1. Breast Cancer Receptors.

Breast cancer molecular subtypes were introduced in 2000 in an attempt to explain the differences in clinical outcomes and response to treatment among breast cancer patients (Perou et al., 2000). The molecular subtypes of breast cancer can be inferred from the previously described three receptors (ER, PR and HER2). The molecular subtype of breast cancer along with other criteria like tumor size, stage, grade and histologic type, affect patients' management and prognosis (Coates et al., 2015; Vuong et al., 2014). Where, identifying the cancer's unique receptors, resulted in applying the active treatment to block the recognized receptors (Schettini et al., 2016).

In clinical routine, the classification of molecular subtypes of breast cancer relies on genomic analysis of biopsy specimens, which is costly and time consuming. Several studies have tried to link certain features of breast cancer detected on various imaging modalities including breast MRI with the molecular subtypes of the tumor in an attempt to non-invasively evaluate the molecular biology of the tumor which has an impact on selecting patients for specific targeted therapies with the potential of improving overall survival. Human perceived imaging features have the advantage of being easily incorporated into clinical practice. Nevertheless, the range of features is constrained, and even established features exhibit inter-observer variability (Grimm et al., 2015).

Artificial intelligence (AI) is the focus of ongoing research in breast cancer detection, classification and management. Several studies showed promising results for incorporation of AI tools into breast cancer imaging algorithms. AI models have been introduced for prediction of malignancy in breast masses depending on certain features extracted from dynamic contrast enhanced MRI (Militello et al., 2022). Others researchers utilized deep learning models for prediction of sentinel lymph node in cases of proved breast cancer to facilitate surgical planning and for prediction of overall prognosis and disease-free survival in treated breast cancer patients (Dong et al., 2018; Park et al., 2018).

The molecular subtype characterization has been the standard practice for treating breast cancer. Early research on breast cancer subtype classification methods used traditional machine learning methods. Recently, there have been several studies for determining the breast cancer molecular subtypes preoperatively that can facilitate and improve individualized treatment plan. Zhang et al. (2021) compared the effectiveness of CNN and convolutional long short term memory (CLSTM) to distinguish between three molecular subtypes of breast cancer: HR, HER2, and triple-negative (TN). A total of 244 DCE-MRI scans were used to train and test the proposed model. The achieved mean accuracies were 91% by CLSTM and 79% by CNN. Li et al. (2019) proposed an approach for classifying molecular subtypes from DCE-MRI breast scans. The region of interest (ROI) of the image was segmented with a dynamic threshold after an accurate annotation of the lesions by an expert radiologist from DCE-MRI. Then, different types of features including texture, morphology, kinetic, and statistics features, were obtained from DCE-MRI to verify the connection between the molecular subtypes and the image phenotypes. Subsequently, recursive feature elimination was applied to find robust and optimal features, as well as improving the performance of the proposed model. Consequently, a total of 637 DCE-MRI slices were used train and test the gradient boosting decision tree classifier, and the achieved recognition precisions for the four molecular subtypes of luminal A, luminal B, HER2, and basal-like were 91%, 89%, 83%, and 87% respectively. Fan et al. (2017) combined the handcrafted features that were derived from DCE-MRI with the clinical information to predict four molecular subtypes of breast cancer: luminal A, luminal B, HER2 and basal-like. A total of 90 characteristics were obtained from DCE-MRI slices, including 2 clinical information-based parameters, and 88 texture features associated with morphology, as well as dynamic features from tumor and background parenchymal enhancement (BPE). These features were reduced to 24 which represented an optimal feature and had high classification performance. A multi-class logistic regression classifier was used to classify

these features and the achieved area under curve (AUC) was 86.9% when classifying a dataset that included 60 DCE-MRI breast scans. Furthermore, the proposed method was validated by using an independent dataset with 36 DCE-MRI breast scans, and the achieved AUC was 87.2%. Yin et al. (2022) proposed an automated model based on using the ResNet18 network to determine the molecular subtypes of breast cancer before surgery. The assessment included a comparison utilizing three MRI modalities namely, T1 weighted with contrast imaging, apparent diffusion coefficient (ADC) and T2 weighted imaging. Where, T1 weighted with contrast imaging achieved better performance in assessing the breast cancer molecular subtypes with other utilized modalities yielded AUCs from 0.762 to 0.92. Lafcı et al. (2023) investigated the association between the molecular subtypes of breast and radiomic features of DCE-MRI of patient with invasive breast cancer. Forty-three radiomic features were extracted using the LIFEX software. The maximum yielded accuracy and AUC were 69.4% and 74.6% respectively. The study by Militello et al. (2023) proposed various machine learning models for predicting coronary artery impairment using radiomics features extracted from Pericoronary adipose tissue features. This study allowed for the implementation of a dependable system that supports cognitive and decision-making processes in the medical field. The extracted radiomic features, as opposed to conventional methods that only use clinical features, allowed for a consistent increase in classification rates. Experimental results showed that using radiomic features alone outperforms using clinical features alone, and that using both clinical and radiomic biomarkers together further enhances the predictive power of the models. The amount of data that was available was this study's main drawback.

Most of previous studies used a single post-contrast MRI among the multiple DCE-MRI of the breast. The first post-contrast of DCE-MRI is the most effective and desirable dynamic for diagnosing breast cancer (Khan et al., 2022). Therefore, the combination of pre-contrast and post-contrast MRI dynamics may be helpful to improve the molecular subtype's classification of breast cancer, and this represents the main motivation for developing this study.

2. Material and method

The proposed model investigates the efficacy of the CNN to extract the deep features from breast DCE-MRI dynamics, the most advised MRI sequences for identifying pathologic breasts. Radiant Software were used to recognize the coordinates of the ROI. Four deep features vectors were combined and utilized to train the SVM classifier. Fig. 2 displays the experimental procedures applied in the current study.

2.1. DCE-MRI dataset

This study aims to classify the molecular subtypes of breast cancer in a dataset of 922 patients at Duke University Hospital in USA (Saha et al., 2018). Only histopathology proven malignant DCE-MRI patients with a clear boundary of mass lesions were chosen for the study, also additional patients who did not meet the inclusion criteria, such as patients who received chemotherapy or hormonal therapy were excluded. With dedicated four-channel breast array coils, 1.5 T and 3 T systems (GE medical system and Siemens) were used for all breast DCE-MRI scans. The proposed system was trained with a total of 149 breast cancer MRI studies, including 74 (49.6%) cases with positive hormone receptors (ER and/or PR), 29 (19.5%) cases with positive HER2 receptors, and 47 (31.5%) cases with triple negative cancers. Additionally, the region of interest (ROI) around the breast lesion was outlined manually by a consultant radiologist to confirm the provided annotations of the downloaded dataset.

2.2. DCE-MRI breast image preprocessing

For the proposed approach, the downloaded dataset was obtained using various imaging equipment with different pixel spacing and spatial resolutions Bilinear interpolation was used to scale all breast DCE-MRI scans to the same spatial resolution (Zhu et al., 2019). Additionally, a major con of MRI compared to other medical imaging modalities is the fact that its intensities are not standardized and vary between the same and consecutive MRI slices due to MRI scanners. Additionally, even though the acquisition protocols for the MRI data from the various scanners were the same, the dynamic intensity range of the MRI slices varied (Hasan & Meziane, 2016; Hasan et al., 2017). Therefore, to reduce the effects of inter-scan and intra-scan variations in the intensity of DCE-MRI, all MRI slices were normalized using histogram normalization (Al-Shamasneh & Ibrahim, 2023; Hasan et al., 2022).

To avoid confounding contributions from noncancerous voxels, a region of interest (ROI) around each breast lesion was cropped from all breast DCE-MRI slices by an experienced radiologist (N. K. Al-Waely) with 10 years of experience in breast cancer diagnosis. The ROI was defined by measuring the longest diameter of each breast lesion and usually was ranged from 20 to 30 pixels, as well as 5 pixels were added around the lesion to include the parenchyma. The selection of ROIs were undergone to the set of criteria; the non-enhanced regions such as the edge of the lesions, bleeding, necrosis, cystic degeneration and blood vessels in the tumor were avoided as much as possible (Hasan et al., 2023; Zhu et al., 2022; Zhu et al., 2019), as shown in Fig. 3. The data set was additionally expanded by transforming and rotating the ROIs

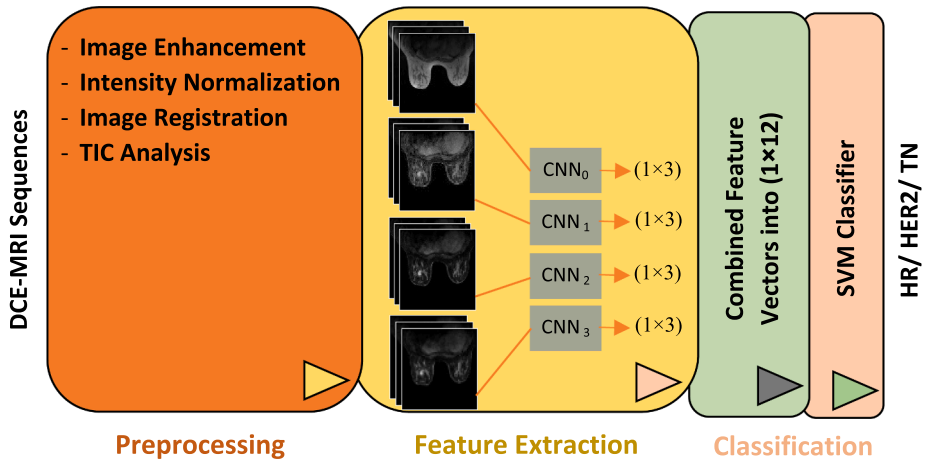

Fig. 2. Proposed model.

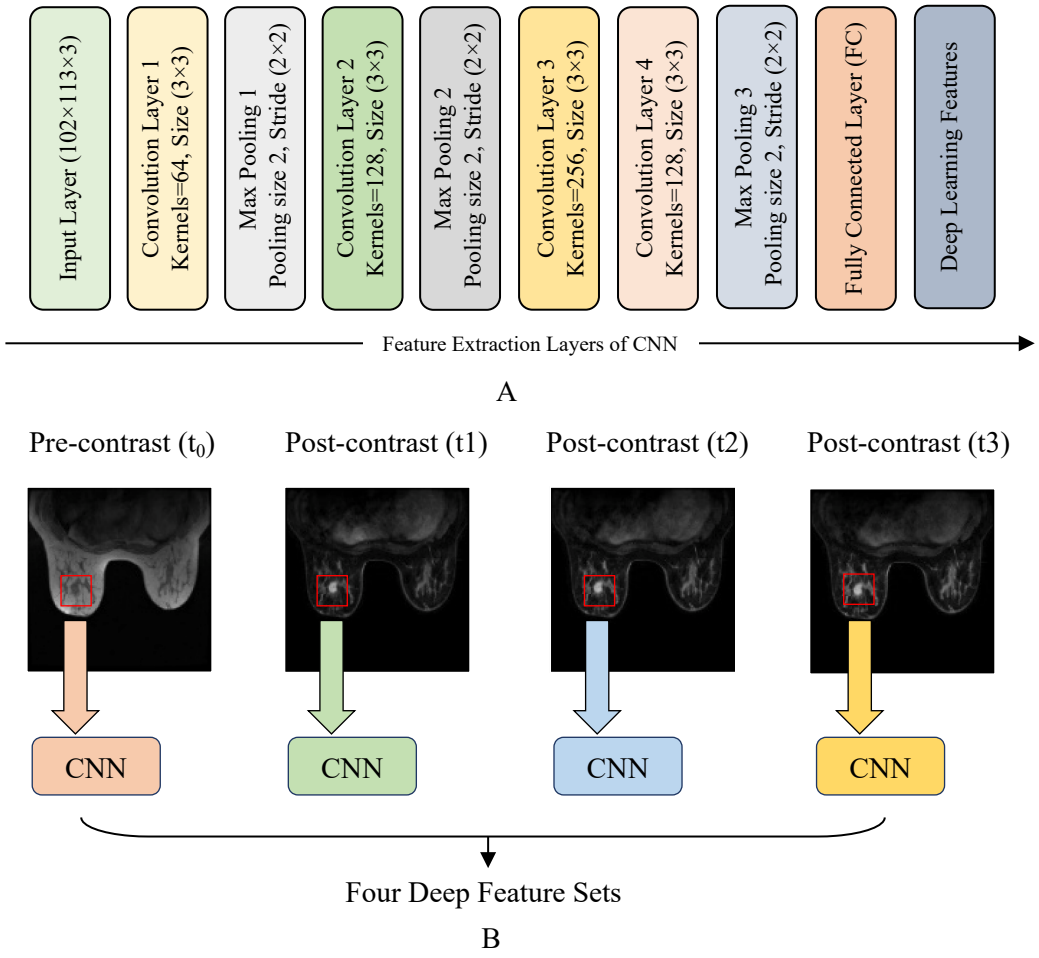

Fig. 3. ROI segmentation example.

images to increase the training size. After augmentation, a total of 1359 ROI images, including 402 ROIs images with positive hormone receptors, 499 ROIs images with positive HER2 receptors, and 458 ROIs images with triple negative cancers. Finally, all ROIs were resized by padding with zeros because the deep learning model does not allow for variation in the input size of MRI slices.

2.3. Conventional CNN feature extraction

CNNs have been proven to be effective when employed for features extraction in a variety of domains, including healthcare, and computer vision, and were used to improve the classification accuracies (Alrubaie et al., 2023; Hasan, AL-Jawad, et al., 2020; Hasan, Jalab, et al., 2020). There are two crucial components of the CNN model: the feature learning (convolutional and pooling layers) and the classification component (fully connected layers) (Govindaswamy et al., 2020). The convolutional layer composes several convolutional filters. These filters convolve around the input image by moving with a step size named stride. Where, the stride can be changed according to the need of the problem (Gu et al., 2018; Hasan, AL-Jawad, et al., 2020). After each convolutional layer, the dimensions of the input image are decreased due to stride process. Therefore, to retrieve the original spatial dimensions of input volume, zero-padding is used to pad the input volume with zeros. Then, applying an element-wise nonlinear activation function on the obtained feature map through the rectified linear unit (ReLU) layer (Gu et al., 2018). Subsequently, the rectified feature map is passed through the pooling layer for dimensionality (Hasan et al., 2019; Lundervold & Lundervold, 2019). Moreover, the max-pooling function is used to determine the maximum number in every sub-region of the feature maps. A batch normalization layer is used to regulate and speed the training process of CNN by normalizing the produced feature maps (Hasan et al., 2019). While, the final fully connected layer is used to take the feature map from the last convolutional layer and apply weights to predict the correct label (Hasan et al., 2019). The Adam optimizer is used to decrease the error function of CNN, and produced an extremely improved weight when the learning rate was set to 0.001.

The extremely efficient CNN architecture is based on how the convolutional layers are connected and how the proper weights are set. The proposed CNN architecture for this specific task, included four-convolutional layers and three pooling layers, as illustrated in Fig. 4-A. The ROI images that were extracted from pre-contrast at t_0 and post-contrast at (t_1, t_2, and t_3 respectively), was fed independently to the proposed CNN. The total of four deep feature subsets of size (1359 × 3), were extracted from every breast DCE-MRI (pre-contrast and post-contrast dynamics of MRI), as shown in Fig. 4-B. Consequently, these subsets were combined into a single feature vector of size (1359 × 12), and fed to the classification stage.

3. Experimental results

In this study, a total of 1359 malignant breast multiple dynamic MRI slices were used to generate sufficient features for classification. The average size of breast malignant lesions was 22 mm^3 (range, 10–65 mm^3). Using 30% of the breast DCE-MRI slices, classification performance was evaluated, and the remaining 70% were used for training. Due to a variety of factors, such as MR hardware and tissue properties

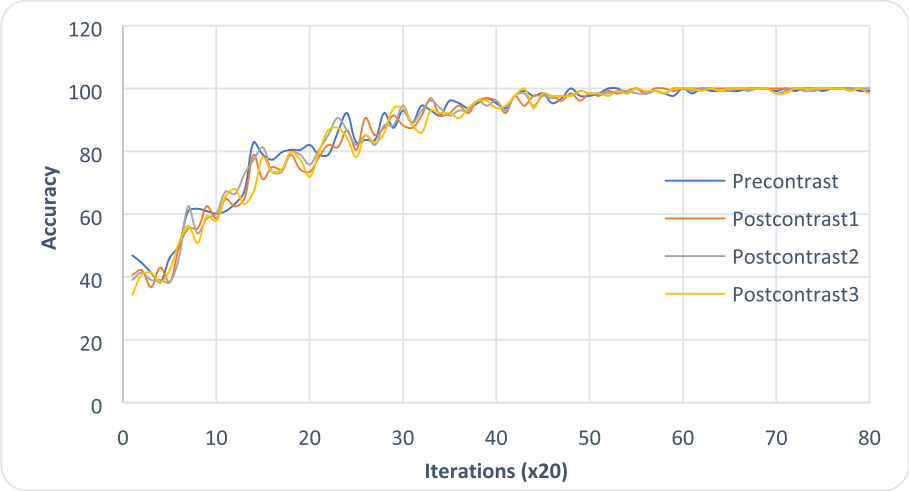

Fig. 4. Deep feature extraction using CNN, (A) Diagram representation of CNN feature extraction layers, (B) Proposed structure of deep feature extraction from DCE-MRI phases.

that could conceal normal or abnormal structures and occasionally simulate diseases or conditions, the signal intensity of DCE-MRI is susceptible to spurious findings, which could result in missed or incorrect diagnoses. Additionally, a large variation in signal intensity may come from utilizing different scanners. Therefore, all breast DCE-MRI scans were enhanced, and the signal intensity was calibrated by implementing an intensity normalization algorithm in the pre-processing step. Then, a rectangular box, which represented a ROI, was drawn by an expert radiologist to cover completely the breast cancer and followed by implementing a zero padding to standardize dimensions of all ROIs according to the largest ROI.

The test results demonstrate the effectiveness of the suggested CNN, that was used to extract deep features from the cropped pre-contrast image which is essential for analysis and comparison, and post-contrast (1st, 2nd, and 3rd) images which are essential for diagnosing and predicting response to therapy (Khan et al., 2022). In this study, the size of deep feature vector from each breast DCE-MRI scan, including one pre-contrast MRI image and three post-contrast MRI images, was 12. The proposed CNN comprised nine layers as described in Table 1. The following parameters were used to train the proposed CNN; the maximum number of epochs is 20, the minimum batch size is 64, the maximum number of iterations is 1400, and the momentums are 0.9 with a learning rate of 0.0001. Fig. 5 shows the training progress plots of the proposed CNN that has a good performance in obtaining the DF from breast single pre-contrast and three post-contrast MRI dynamics.

The performance of the deep features that are extracted from DCE-MRI dynamics to distinguish between three different types of breast cancer on DCE-MRI, is evaluated by comparing the following metrices: TP, TN, FP, and the FN. Additionally, four more matrices are considered to evaluate the proposed model; accuracy (ACC), area under curve (AUC), sensitivity (SEN), and specificity (SPE). Where, the SEN and SPE

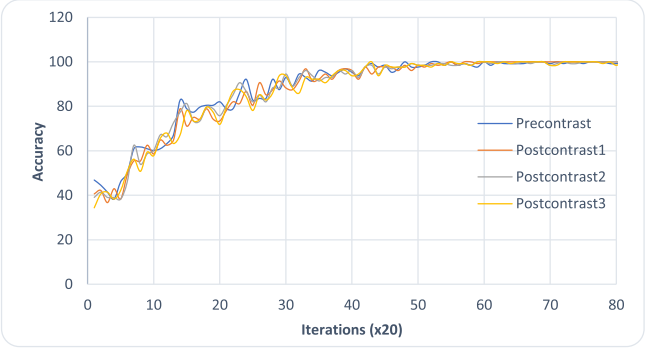

Fig. 5. The training plots of the proposed CNN on pre-contrast and post-contrast at (t_1, t_2, and t_3 respectively).

indicate the ability of the proposed model to correctly diagnose molecular subtypes of breast cancer. The experimental results depicts that the extracted deep features from pre-contrast and post-contrast of MRI dynamics, improved the efficacy of diagnosing the molecular subtypes of breast cancer, when combined into a single vector. Among the multiple DCE dynamics, most of previous studies focused on using a single post-contrast MRI that is especially the first MRI dynamic. Whereas the experimental results shows that the combination of pre and post-contrast MRI dynamics was superior to individual MRI dynamic, and achieved the best predicting response using the SVM classifier with a highest ACC and AUC values of 99.78% and 100% respectively, as illustrated in Table 2.

The utilization of the pre-trained model was motivated by its

Table 1
The proposed architecture of CNN.

Layer Name	Kernel filter	Kernel Size	Feature Map
Input layer		(102 × 113)	
Convolution layer 1	64	(3 × 3)	(102 × 113 × 64)
Pooling layer 1		(2 × 2)	(51 × 56 × 64)
Convolution layer 2	128	(3 × 3)	(51 × 56 × 128)
Pooling layer 2		(2 × 2)	(25 × 28 × 128)
Convolution layer 3	256	(3 × 3)	(25 × 28 × 256)
Convolution layer 4	128	(3 × 3)	(25 × 28 × 128)
Pooling layer 3		(2 × 2)	(12 × 14 × 128)
Fully connected layer		(1 × 3)	(1 × 3)

Table 2
Achieved results by the proposed CNN as a feature extractor using SVM classifier.

Features	DF-Pre-contrast	DF-Post-contrast 1	DF-Post-contrast 2	DF-Post-contrast 3	Combined Features
Accuracy	99.63	99.34	99.04	98.90	99.78
TP	398	394	393	392	399
TN	956	956	953	952	957
FP	11	1	3	3	0
FN	4	8	10	12	3
Sensitivity	99.00	98.01	97.51	97.02	99.25
Specificity	99.90	99.9	99.68	99.58	100
AUC	100	100	100	100	100

performance on many medical tasks such as AlexNet (Russakovsky et al., 2015), SqueezeNet (Iandola et al., 2016) and GoogLeNet (Zhou et al., 2016). Therefore, in this study the acquired knowledge of these pre-trained models is exploited to extract feature from pre-contrast and post-contrast MRI dynamics of the utilized dataset and compared their performances with the proposed CNN in this study, as presented in Table 3. Accordingly, AlexNet is composed of 5 convolutional layers ending with 3 fully connected layers (Yuan & Zhang, 2016). While, SqueezeNet includes 18 squeeze convolutional layer and 1000 classes in the output layer (Elharrouss et al., 2022). Moreover, GoogleNet includes 22 convolutional layers with 27 pooling layers and 1000 classes in the output layer (Zhou et al., 2016). When comparing the achieved results of the existing methods with the proposed CNN, the proposed method is better than the pre-trained networks in terms of the average classification accuracy, feature dimensions, and number of layers. Where, the maximum achieved accuracy of 99.78 is achieved by using feature vector of 12 predictors, and network of 9 layers.

Additionally, ANOVA (one-way analysis of variance) is used to evaluate the discriminatory power of the extracted deep features based on the F-statistic and P-value. The F-statistic, which is used to determine whether the ratio of these variance estimates is significantly greater than 1, is described as a ratio between-group variance to within-group variance (Hasan & Meziane, 2016). Where, larger F-statistic indicates the differences between-group variance is larger than within-group variance. This can be interpreted that there is a statistically significant difference in the group means. P-value, on the other hand, is the probability that the test statistic will be at least equal to or less than the test's critical value (5% or 1%). The feature will be significant if the P-value for the larger F-statistic value is lower than the critical value (Kim, 2017). Table 4 shows that all the extracted features have P-values that are less than 0.0001. This indicates that all the extracted features are significant but from the associated F-statistics show that the degree of significance are varied among the extracted features. Where, some of the extracted features have large F-statistics such as predictor 2 and predictor 3 that were extracted from pre-contrast MRI, and some of the extracted features have small F-statistics such as predictor 3 from post-contrast at t_2 and t_3 MRI respectively. Although, the highest accuracy (99.78%) was achieved by combining the extracted features from pre and post contract MRI dynamics, the achieved accuracy by using only the pre-contrast is also high (99.63%) and decreased by (0.15%) from the highest accuracy, as demonstrated in Table 3. Thus, the pre-contrast of breast MRI can be utilized efficiently to classify the molecular subtypes of breast cancer. Classifying the molecular subtypes without the need for administering gadolinium contrast would have a great impact on the management of patients with breast cancer as it would decrease the cost burden on the patient, decrease the time of MRI exam, increase the number of patients that can be examined per day and eliminate the potential side effects after administering the MRI contrast agent like allergy, headache and nausea (Behzadi et al., 2018).

Table 4
ANOVA test to determine the significance of the extracted features among pre- and post-contrast dynamics.

Deep Features	F-Statistics	P-value
Pre-contrast (t_0)		
Predictor 1	103.8	<0.0001
Predictor 2	1215.5	<0.0001
Predictor 3	1223.2	<0.0001
Post-contrast (t_1)		
Predictor 1	114.9	<0.0001
Predictor 2	99.1	<0.0001
Predictor 3	60.7	<0.0001
Post-contrast (t_2)		
Predictor 1	91.8	<0.0001
Predictor 2	143.5	<0.0001
Predictor 3	49.3	<0.0001
Post-contrast (t_3)		
Predictor 1	69.8	<0.0001
Predictor 2	83.8	<0.0001
Predictor 3	43.2	<0.0001

Furthermore, patients with certain types of breast cancers are treated with chemotherapy prior to definitive surgery and it has been shown that the hormone receptor status which defines the molecular subtype may change during the time course of such treatment (Niikura et al., 2012; Niikura et al., 2016). Thus, assessment of the molecular type in residual or recurrent breast cancer by non-enhanced MR exam without the need for multiple invasive biopsies or frequent administrations of gadolinium contrast would permit more tolerable and efficient management plan for the patient.

3.1. Comparison with existing state-of-the art

To validate the effectiveness of the proposed method, Table 5 summarizes previous studies that investigated the molecular subtype's classification of DCE-MRI breast cancer. Zhang et al. (2021) study was developed to distinguish between three breast cancer molecular subtypes using deep learning algorithms such as CNN and a recurrent CNN. The achieved accuracies of CNN and CLSTM were 79% and 91% respectively when evaluated with 244 DCE-MRI breast scans. Li et al. (2019) proposed a method for identifying molecular subtypes from phenotypes in DCE-MRI breast images using radiomics. Texture, dynamic kinetics, morphology and statistics features were among the

Table 3
Comparisons using the same breast DCE-MRI dataset.

Methods	DF-Pre-contrast	DF-Post-contrast 1	DF-Post-contrast 2	DF-Post-contrast 3	Combined Features
AlexNet (Russakovsky et al., 2015)					
Accuracy	91.04	90.86	87.95	86.55	92.62
Features Dimensions	4096	4096	4096	4096	16,384
SqueezeNet [33]					
Accuracy	93.95	93.44	91.54	89.88	94.51
Features Dimensions	1000	1000	1000	1000	4000
GoogLeNet (Zhou et al., 2016)					
Accuracy	90.23	89.33	85.11	82.34	90.38
Features Dimensions	1000	1000	1000	1000	4000
Proposed CNN					
Accuracy	99.63	99.34	99.04	98.90	99.78
Features Dimensions	3	3	3	3	12

Table 5
Comparison of the proposed model with other models of molecular subtype's classification.

References	Dataset	Methods	Accuracy	AUC
Zhang et al. (2021)	244	- CNN - CLSTM	79% 91%	86.6% 91.4%
Li et al. (2019)	637	- Texture features. - Statistical features. - Morphological features. - Kinetics features.	87%	87%
Fan et al. (2017)	96	- Texture features. - Morphological features. - First-order statistics. - Dynamic features.	-	86.9%
Yin et al. (2022)	136	- ResNet18	-	76.2% to 92%
Lafcı et al. (2023)	73	- Radiomic features. . Conventional. Histogram. Shape. GLCM. GLRLM. GLZLM. NGLDM	69.4%	74.6%
Proposed method	1359	- CNN	99.78%	100%

features that were taken into consideration. The achieved accuracy was 87% when evaluated with 637 DCE-MRI scans. Fan et al. (2017) studied the role of features derived from DCE-MRI and incorporated clinical information such as the age and menopausal status, to predict the molecular subtypes of breast cancer.

The results of predication model revealed that the achieved overall classification performance with an AUC value was 86.9%. Yin et al. (2022) investigated the efficacy of multi-parametric MRI-based CNN for the preoperative assessment of breast cancer molecular subtypes. The yielded AUC values were between 76.2% and 92%, for separating each molecular subtypes of breast cancer of a dataset that included 136 DCE-MRI scans. Finally, Lafcı et al. (2023) studied the association between the molecular subtypes of breast cancer and radiomic features of DCE-MRI scans. The maximum achieved accuracy and AUC were 69.4% and 74.6% respectively when classifying a dataset of 73 DCE-MRI scans.

The accuracy of the suggested method performed better than that of earlier studies. This demonstrates that the proposed CNN is effective in extracting the most efficient features that can be used for identifying the molecular subtypes of breast cancer by utilizing DCE-MRI modality. Furthermore, the proposed method succeeded in discriminating the three intrinsic molecular subtypes of the breast accurately from only the pre-contrast phase without need for gadolinium injection. This could be a helpful auxiliary tool to help radiologists interpret DCE-MRI scans in their own subjective way, and help to diagnose patients who have severe allergic to gadolinium-based contrast media.

4. Conclusion

In this study, a new CNN model was proposed for the extraction of efficient features from DCE-MRI of the breast after being analyzed by radiologists in a preprocessing stage. The experimental results depict that the proposed model may significantly enhance DCE-MRI's capability to identify the molecular subtypes of breast cancer. Additionally, the recent studies showed that the administered gadolinium accumulates with higher concentrations in certain body tissues including the brain, bone, skin, and liver. Therefore, the potential of the proposed model provides the contrast-free examination with high accuracy by using the deep features of unenhanced breast dynamic of DCE-MRI scan to differentiate among molecular subtypes of breast cancer. However, the manual delineation of ROI from DCE-MRI scans by experienced radiologist represents the main limitation of the proposed model. Thus, we recommend future research focusing on placing the ROI automatically without the need for the human intervention.

CRediT authorship contribution statement

Ali M. Hasan: Software, Writing – review & editing. **Noor K.N. Al-Waely:** Data curation, Visualization. **Hadeel K. Aljobouri:** Data curation. **Hamid A. Jalab:** Software. **Rabha W. Ibrahim:** Methodology, Writing – review & editing. **Farid Meziane:** Investigation, Conceptualization.

Declaration of Competing Interest

The authors declare that they have no known competing financial interests or personal relationships that could have appeared to influence the work reported in this paper.

Data availability

Data will be made available on request.

Acknowledgment

This research is supported by Al-Nahrain University, Project CM-PMP-22-001.

References

Al-Hashimi, M. M. (2021). Trends in breast cancer incidence in Iraq during the period 2000–2019. *Asian Pacific Journal of Cancer Prevention: APJCP, 22*(12), 3889.
Al-Shamasneh, A. A. R., & Ibrahim, R. W. (2023). Image denoising based on quantum calculus of local fractional entropy. *Symmetry, 15*(2), 396.
Alrubaie, H., Aljobouri, H. K., & AL-Jobawi, Z. J., & Çankaya, I.. (2023). Convolutional neural network deep learning model for improved ultrasound breast tumor classification. *Al-Nahrain Journal for Engineering Sciences, 26*(2), 57–62.
Behzadi, A. H., Zhao, Y., Farooq, Z., & Prince, M. R. (2018). Immediate allergic reactions to gadolinium-based contrast agents: A systematic review and meta-analysis. *Radiology, 286*(2), 471–482.
Blink, E. (2004). *Basic mri : Physics*.
Coates, A. S., Winer, E. P., Goldhirsch, A., Gelber, R. D., Gnant, M., Piccart-Gebhart, M., … Senn, H. J. (2015). Tailoring therapies–improving the management of early breast cancer: St Gallen International Expert Consensus on the Primary Therapy of Early Breast Cancer 2015. *Annals of Oncology, 26*(8), 1533–1546. https://doi.org/10.1093/annonc/mdv221
Dong, Y., Feng, Q., Yang, W., Lu, Z., Deng, C., Zhang, L., … Pei, S. (2018). Preoperative prediction of sentinel lymph node metastasis in breast cancer based on radiomics of T2-weighted fat-suppression and diffusion-weighted MRI. *European Radiology, 28*(2), 582–591.
Elharrouss, O., Akbari, Y., Almaadeed, N., & Al-Maadeed, S. (2022). Backbones-review: Feature extraction networks for deep learning and deep reinforcement learning approaches. *arXiv preprint arXiv:2206.08016*.
Fan, M., Li, H., Wang, S., Zheng, B., Zhang, J., & Li, L. (2017). Radiomic analysis reveals DCE-MRI features for prediction of molecular subtypes of breast cancer. *PLoS One1, 12*(2), Article e0171683.
Feng, Y., Spezia, M., Huang, S., Yuan, C., Zeng, Z., Zhang, L., … Luo, W. (2018). Breast cancer development and progression: Risk factors, cancer stem cells, signaling pathways, genomics, and molecular pathogenesis. *Genes & Diseases, 5*(2), 77–106.
Ferris, N., & Goergen, S. (2016). Gadolinium contrast medium (MRI contrast agents). *Inside Radiology website. insideradiology. com. au/gadolinium-contrast-medium/. Updated November, 22*.
Govindaswamy, A. G., Montague, E., Raicu, D. S., & Furst, J. (2020). CNN as a feature extractor in gaze recognition. 2020 3rd Artificial Intelligence and Cloud Computing Conference.
Grimm, L. J., Anderson, A. L., Baker, J. A., Johnson, K. S., Walsh, R., Yoon, S. C., & Ghate, S. V. (2015). Interobserver variability between breast imagers using the fifth edition of the BI-RADS MRI lexicon. *American Journal of Roentgenology, 204*(5), 1120-1124.
Gu, J., Wang, Z., Kuen, J., Ma, L., Shahroudy, A., Shuai, B., … Cai, J. (2018). Recent advances in convolutional neural networks. *Pattern Recognition, 77*, 354–377.
Hasan, A., & Meziane, F. (2016). Automated screening of MRI brain scanning using grey level statistics. *Computers & Electrical Engineering, 53*, 276–291. http://www.sciencedirect.com/science/article/pii/S0045790616300568.
Hasan, A. M., AL-Jawad, M. M., Jalab, H. A., Shaiba, H., Ibrahim, R. W., & AL-Shamasneh, A. A. R. (2020). Classification of Covid-19 coronavirus, pneumonia and healthy lungs in CT scans using Q-deformed entropy and deep learning features. *Entropy, 22*(5), 517.
Hasan, A. M., Al-Waely, N. K. N., Ajobouri, H. K., Ibrahim, R. W., Jalab, H. A., & Meziane, F. (2023). A classification model of breast masses in DCE-MRI using kinetic curves features with quantum-Raina's polynomial based fusion. *Biomedical Signal Processing and Control, 84*, Article 105002. https://doi.org/10.1016/j.bspc.2023.105002

Hasan, A. M., Jalab, H. A., Ibrahim, R. W., Meziane, F., AL-Shamasneh, A. A. R., & Obaiys, S. J. (2020). MRI brain classification using the quantum entropy LBP and deep-learning-based features. *Entropy, 22*(9), 1033.

Hasan, A. M., Jalab, H. A., Meziane, F., Kahtan, H., & Al-Ahmad, A. S. (2019). Combining deep and handcrafted image features for MRI brain scan classification. *IEEE Access, 7*, 79959–79967.

Hasan, A. M., Meziane, F., Aspin, R., & Jalab, H. A. (2017). MRI brain scan classification using novel 3-D statistical features. Proceedings of the Second International Conference on Internet of things, Data and Cloud Computing.

Hasan, A. M., Qasim, A. F., Jalab, H. A., & Ibrahim, R. W. (2022). Breast cancer MRI classification based on fractional entropy image enhancement and deep feature extraction. *Baghdad Science Journal*, 0221.

Iandola, F. N., Han, S., Moskewicz, M. W., Ashraf, K., Dally, W. J., & Keutzer, K. (2016). SqueezeNet: AlexNet-level accuracy with 50x fewer parameters and <0.5 MB model size. *arXiv preprint arXiv:1602.07360*.

Iranmakani, S., Mortezazadeh, T., Sajadian, F., Ghaziani, M. F., Ghafari, A., Khezerloo, D., & Musa, A. E. (2020). A review of various modalities in breast imaging: Technical aspects and clinical outcomes. *Egyptian Journal of Radiology and Nuclear Medicine, 51*(1), 57. https://doi.org/10.1186/s43055-020-00175-5

Kawahara, D., & Nagata, Y. (2021). T1-weighted and T2-weighted MRI image synthesis with convolutional generative adversarial networks. *Reports of Practical Oncology and Radiotherapy, 26*(1), 35–42. https://doi.org/10.5603/RPOR.a2021.0005

Khan, N., Adam, R., Huang, P., Maldjian, T., & Duong, T. Q. (2022). Deep learning prediction of pathologic complete response in breast cancer using MRI and other clinical data: A systematic review. *Tomography, 8*(6), 2784–2795.

Kim, T. K. (2017). Understanding one-way ANOVA using conceptual figures. *Korean Journal of Anesthesiology, 70*(1), 22–26.

Lafcı, O., Celepli, P., Öztekin, P. S., & Koşar, P. N. (2023). DCE-MRI radiomics analysis in differentiating luminal A and luminal B breast cancer molecular subtypes. *Academic Radiology, 30*(1), 22–29.

Lee, J. M., & Houssami, N. (2016). Imaging surveillance of women with a personal history of breast cancer. In *Breast Cancer Screening* (pp. 299–322). Elsevier.

Li, W., Yu, K., Feng, C., & Zhao, D. (2019). Molecular subtypes recognition of breast cancer in dynamic contrast-enhanced breast magnetic resonance imaging phenotypes from radiomics data. *Computational and Mathematical Methods in Medicine, 2019*.

Lundervold, A. S., & Lundervold, A. (2019). An overview of deep learning in medical imaging focusing on MRI. *Zeitschrift für Medizinische Physik, 29*(2), 102–127.

Militello, C., Prinzi, F., Sollami, G., Rundo, L., La Grutta, L., & Vitabile, S. (2023). CT radiomic features and clinical biomarkers for predicting coronary artery disease. *Cognitive Computation, 15*(1), 238–253. https://doi.org/10.1007/s12559-023-10118-7

Militello, C., Rundo, L., Dimarco, M., Orlando, A., Woitek, R., D'Angelo, I., … Bartolotta, T. V. (2022). 3D DCE-MRI radiomic analysis for malignant lesion prediction in breast cancer patients. *Academic Radiology, 29*(6), 830–840. https://doi.org/10.1016/j.acra.2021.08.024

Niikura, N., Liu, J., Hayashi, N., Mittendorf, E. A., Gong, Y., Palla, S. L., … Ueno, N. T. (2012). Loss of human epidermal growth factor receptor 2 (HER2) expression in metastatic sites of HER2-overexpressing primary breast tumors. *Journal of Clinical Oncology, 30*(6), 593–599.

Niikura, N., Tomotaki, A., Miyata, H., Iwamoto, T., Kawai, M., Anan, K., … Masuoka, H. (2016). Changes in tumor expression of HER2 and hormone receptors status after neoadjuvant chemotherapy in 21 755 patients from the Japanese breast cancer registry. *Annals of oncology, 27*(3), 480–487.

Omer, H. K., Jalab, H. A., Hasan, A. M., & Tawfiq, N. E. (2019). Combination of local binary pattern and face geometric features for gender classification from face images. *2019 9Th IEEE International Conference on Control System, Computing and Engineering (ICCSCE)*.

Park, H., Lim, Y., Ko, E. S., Cho, H.-H., Lee, J. E., Han, B.-K., … Park, K. W. (2018). Radiomics signature on magnetic resonance imaging: Association with disease-free survival in patients with invasive breast cancer. *Clinical Cancer Research, 24*(19), 4705–4714.

Perou, C. M., Sørlie, T., Eisen, M. B., Van De Rijn, M., Jeffrey, S. S., Rees, C. A., … Akslen, L. A. (2000). Molecular portraits of human breast tumours. *Nature, 406*(6797), 747–752.

Russakovsky, O., Deng, J., Su, H., Krause, J., Satheesh, S., Ma, S., … Bernstein, M. (2015). Imagenet large scale visual recognition challenge. *International Journal of Computer Vision, 115*(3), 211–252.

Saha, A., Harowicz, M. R., Grimm, L. J., Kim, C. E., Ghate, S. V., Walsh, R., & Mazurowski, M. A. (2018). A machine learning approach to radiogenomics of breast cancer: A study of 922 subjects and 529 DCE-MRI features. *British Journal of Cancer, 119*(4), 508–516.

Schettini, F., Buono, G., Cardalesi, C., Desideri, I., De Placido, S., & Del Mastro, L. (2016). Hormone Receptor/Human Epidermal Growth Factor Receptor 2-positive breast cancer: Where we are now and where we are going. *Cancer Treatment Reviews, 46*, 20–26. https://doi.org/10.1016/j.ctrv.2016.03.012

Sung, H., Ferlay, J., Siegel, R. L., Laversanne, M., Soerjomataram, I., Jemal, A., & Bray, F. (2021). Global cancer statistics 2020: GLOBOCAN estimates of incidence and mortality worldwide for 36 cancers in 185 countries. *CA: A Cancer Journal for Clinicians, 71*(3), 209–249.

Ulas, C., Das, D., Thrippleton, M. J., Valdes Hernandez, M. D. C., Armitage, P. A., Makin, S. D., Wardlaw, J. M., & Menze, B. H. (2019). Convolutional neural networks for direct inference of pharmacokinetic parameters: Application to stroke dynamic contrast-enhanced MRI. *Frontiers in Neurology, 9*, 1147.

Vuong, D., Simpson, P. T., Green, B., Cummings, M. C., & Lakhani, S. R. (2014). Molecular classification of breast cancer. *Virchows Archiv, 465*(1), 1–14. https://doi.org/10.1007/s00428-014-1593-7

Yin, H., Bai, L., Jia, H., & Lin, G. (2022). Noninvasive assessment of breast cancer molecular subtypes on multiparametric MRI using convolutional neural network with transfer learning. *Thoracic Cancer, 13*(22), 3183–3191.

Yuan, Z.-W., & Zhang, J. (2016, 2016/08/29). *Feature extraction and image retrieval based on AlexNet* https://proceedings.spiedigitallibrary.org/proceeding.aspx?articleid=2547824 10.1117/12.2243849.

Zhang, Y., Chen, J.-H., Lin, Y., Chan, S., Zhou, J., Chow, D., … Wang, X. (2021). Prediction of breast cancer molecular subtypes on DCE-MRI using convolutional neural network with transfer learning between two centers. *European Radiology, 31*(4), 2559–2567.

Zhao, H., Zou, L., Geng, X., & Zheng, S. (2015). Limitations of mammography in the diagnosis of breast diseases compared with ultrasonography: A single-center retrospective analysis of 274 cases. *European Journal of Medical Research, 20*(1), 49. https://doi.org/10.1186/s40001-015-0140-6

Zhou, B., Khosla, A., Lapedriza, A., Torralba, A., & Oliva, A. (2016). Places: An image database for deep scene understanding. *arXiv preprint arXiv:1610.02055*.

Zhu, J.-J., Shen, J., Zhang, W., Wang, F., Yuan, M., Xu, H., & Yu, T.-F. (2022). Quantitative texture analysis based on dynamic contrast enhanced MRI for differential diagnosis between primary thymic lymphoma from thymic carcinoma. *Scientific Reports, 12*(1), 12629. https://doi.org/10.1038/s41598-022-16393-y

Zhu, Z., Albadawy, E., Saha, A., Zhang, J., Harowicz, M. R., & Mazurowski, M. A. (2019). Deep learning for identifying radiogenomic associations in breast cancer. *Computers in Biology and Medicine, 109*, 85–90.